

Ag/Polypyrrole Core–Shell Nanostructures: Interface Polymerization, Characterization, and Modification by Gold Nanoparticles

Xiaomiao Feng, Haiping Huang, Qingqing Ye, Jun-Jie Zhu,* and Wenhua Hou*

School of Chemistry and Chemical Engineering, Key Laboratory of Analytical Chemistry for Life Science, Key Laboratory of Mesoscopic Chemistry, Nanjing University, Nanjing 210093, People's Republic of China

Received: February 10, 2007; In Final Form: March 19, 2007

Polypyrrole (PPy)-coated Ag composites were synthesized through an immiscible organic/inorganic biphasic system in the presence of polyvinylpyrrolidone (PVP). Highly dispersed PPy/Ag was obtained by using interface polymerization and controlling the reactive conditions. The presence of PVP could realize the effective coating of PPy on the surface of Ag. The core–shell structure was directly confirmed by transmission electron microscopy and also characterized by techniques such as Fourier transform infrared spectroscopy and X-ray diffraction. Furthermore, three-layered Au-modified PPy-coated Ag nanocomposite was prepared through the reaction of Au colloidal solution and PPy/Ag. Moreover, Au/PPy/Ag nanocomposite was immobilized on the surface of a glassy carbon electrode and applied to construct a dopamine (DA) biosensor. The biosensor exhibited a fast amperometric response to DA with the linear range from 1×10^{-4} to 5×10^{-3} mol/L.

Introduction

Nanocomposites exhibit improved physical and chemical properties over their single-component counterparts and are potentially useful in a broad range of applications.¹ Polypyrrole (PPy) is known as one of the most important conducting polymers due to its high conductivity, ease of preparation, good environmental stability, and a large variety of applications.² The embedment of metallic or semiconducting nanoparticle (NP) cores inside of conducting polymers, such as PPy³ and polyaniline,⁴ is of interest because of the strong electronic interaction between the NPs and polymer matrixes. For example, Au/PPy core–shell NPs have been synthesized by polymerization of pyrrole on the surface of gold⁵ and through the redox reaction between HAuCl₄ and pyrrole using a special diblock copolymer as stabilizer.³ Ag–PPy coaxial nanocables have been fabricated through the redox reaction of silver nitrate and pyrrole with the help of assistant agent.⁶ Sarma et al. synthesized a PANI/Au composite with a significantly higher electrical conductivity than that of PANI alone.⁷

The methods to synthesize conducting polymers have been developed both chemically and electrochemically through the polymerization of monomer with the aid of an external “hard template” such as aluminosilicate MCM-41, the channels of microporous membranes and porous alumina, and an external “soft template” such as liquid crystalline phases, micelles, and reverse microemulsion.⁸ The main advantage of the method is that the length and diameter of the products can be controlled by the selected porous membrane, but the removal of the template is tedious when hard templates are employed. A novel seeding method has been reported to synthesize polyaniline nanostructures that requires very small amount of seeds of nanofibers, regardless of their chemical nature, which results in a precipitate with bulk fibrillar morphology.⁹ Liu et al. reported a general templateless assembly of large arrays of oriented nanowires containing molecularly aligned conducting

polymer.¹⁰ Recently, a different method has been reported for the synthesis of conducting polymer nanofibers at the interface of an immiscible organic/inorganic biphasic system.¹¹ According to the report, interface polymerization has many advantages, e.g., the synthesis and purification are simple without template-removing steps and the prepared samples are readily dispersed in water that facilitates the biological applications.

Herein, we report the synthesis of PPy-coated Ag nanocomposite by using the redox reaction of silver nitrate and pyrrole via interface polymerization in the presence of PVP. Furthermore, the obtained PPy-coated Ag composite was modified by Au colloidal NPs to give rise to a three-layered Au/PPy/Ag structure. On the basis of the good biocompatibility of Au and the electrical properties of PPy, Au/PPy/Ag was applied to construct a dopamine (DA) biosensor. The Au/PPy/Ag-modified electrode showed an enhanced electrocatalytic activity for the oxidation of DA compared with that of the PPy/Ag-modified electrode. The morphology and composition of PPy/Ag and Au/PPy/Ag were investigated in detail by some techniques such as transmission electron microscopy (TEM), Fourier transform infrared spectroscopy (FTIR), UV–vis, and X-ray diffraction (XRD). The possible formation mechanism and the effect of experimental conditions on the resulting composites are also discussed.

Experimental Section

Materials. Pyrrole was purchased from Aldrich, and silver nitrate (AgNO₃), carbon tetrachloride (CCl₄), sulfuric acid (H₂SO₄), and polyvinylpyrrolidone (PVP) were purchased from Shanghai Chemical Reagent Company. Pyrrole monomer was distilled under reduced pressure, and other reagents were used as received without further treatment.

Preparation of PPy-Coated Ag Nanocomposite. In a typical procedure for the synthesis of PPy-coated Ag nanocomposite, 1 mmol of pyrrole was dissolved in 10 mL of organic phase (CCl₄). A certain amount of AgNO₃ and PVP was dissolved in 10 mL of distilled water. The two solutions were then carefully

* Corresponding authors. E-mail: jjzhu@nju.edu.cn (J.-J.Z.); whou@nju.edu.cn (W.H.). Phone and Fax: +86-25-83594976.

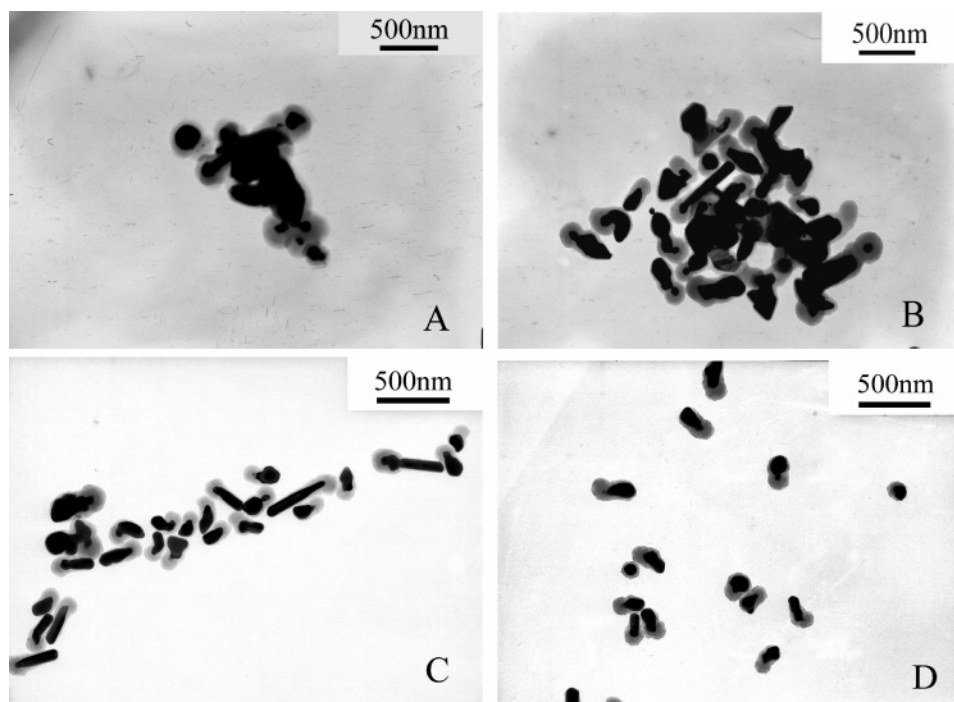


Figure 1. TEM images of PPy-coated Ag composites prepared at different PVP concentrations: (A) 0.2%, (B) 0.5%, (C) 1%, and (D) 2%. Synthetic conditions: pyrrole 1 mmol; AgNO₃ 0.12 g; reaction time 48 h; room temperature.

transferred to a beaker, and an interface was generated immediately between two layers. Brownish black PPy-coated Ag nanocomposite was first formed at the interface and then gradually diffused into the whole aqueous phase. The reaction was allowed to proceed for 48 h. After the reaction, the upper layer mixture was centrifuged, and the precipitate was washed with distilled water and ethanol for several times, respectively. The final product was dried in vacuum at 40 °C for 24 h.

Preparation of Au-Modified PPy-Coated Ag Composite. The Au colloid was prepared according to the reported method by boiling HAuCl₄ aqueous solution with trisodium citrate.¹² The average diameter of the prepared Au NPs is about 30 nm. PPy-coated Ag nanocomposite was added to the Au colloid at a concentration of 1.0 mg/mL under stirring. The reaction was allowed to proceed for 12 h, and the resultant product was centrifuged and dried. Au NPs could be adsorbed on the surface of PPy, leading to the formation of Au-modified PPy-coated Ag composite.

Preparation of Au/PPy/Ag-Modified Glassy Carbon Electrodes. The glassy carbon electrodes (GCE, 3 mm in diameter) were polished with 1.0, 0.3, and 0.05 μm alumina slurry followed by rinsing with doubly distilled water and drying at room temperature. Au/PPy/Ag was dispersed in distilled water to form a 1.0 mg/mL solution and ultrasonically treated for 30 min. The colloidal solution (5 μL) was dropped onto the pretreated GCE surface and allowed to dry under ambient conditions.

Characterization. The morphologies of Au/PPy/Ag and PPy/Ag composites were observed by TEM (JEOL JEM-200CX). X-ray diffraction patterns were taken on a Philip-X'Pert X-ray diffractometer with a Cu Kα X-ray source. UV-vis absorption spectra of Au/PPy/Ag and PPy/Ag dispersed in distilled water through ultrasonic irradiation were recorded on a UV-2401PC spectrometer. All FTIR spectroscopic measurements were performed on a Bruker model VECTOR22 Fourier transform spectrometer using KBr pressed disks. The amount of Au within the composite was determined by thermogravimetric analysis (TGA) on a Shimadzu TGA-50 instrument from room temper-

ature to 800 °C at a heating rate of 10 °C/min in an air atmosphere. Electrochemical experiments were conducted using a CHI660B workstation (from Shanghai Chenhua, Shanghai) in a three-electrode system. All electrochemical experiments were performed in a cell containing 20.0 mL of pH 1 H₂SO₄ at room temperature and using a coiled platinum wire as the auxiliary, a saturated calomel electrode (SCE) as reference, and the Au/PPy/Ag (PPy/Ag)-modified GCE as a working electrode. All experimental solutions were deaerated by bubbling highly pure nitrogen for 10 min, and a nitrogen atmosphere was kept over the solutions during measurements.

Results and Discussion

PPy-coated Ag nanocomposite was successfully synthesized through the redox reaction of AgNO₃ and pyrrole monomer in the presence of PVP. The reaction was carried out in the interface of CCl₄/H₂O two phases without stirring. The core-shell structure can be confirmed directly by TEM. Figure 1 shows the TEM images of PPy-coated Ag nanocomposites prepared at different PVP concentrations. As shown in Figure 1, the dark spots inside the nanocomposites correspond to Ag that is surrounded by PPy matrix. The PVP concentration has a strong effect on the size and morphology of the resultant products. When the PVP concentrations were 0.2% and 0.5%, the obtained PPy-coated Ag nanocomposite with a diameter in the range of 200–800 nm was conglomerated. When the PVP concentration was increased from 0.5% to 1%, the size of the resultant nanocomposite was about 200–500 nm and the degree of dispersion was improved. At the same time, some one-dimensional structures appeared. The diameter of the PPy-coated Ag nanocomposite was between 150 and 400 nm, and most of nanocomposites obtained had a short rodlike shape when the PVP concentration was 2%. The PPy layer was thick in one end and thin in another end, which might be caused by the interface polymerization. The prepared product with shell thicknesses of 10–150 nm and core diameters of 100–300 nm were uniform in size and well dispersed as regarded in a full

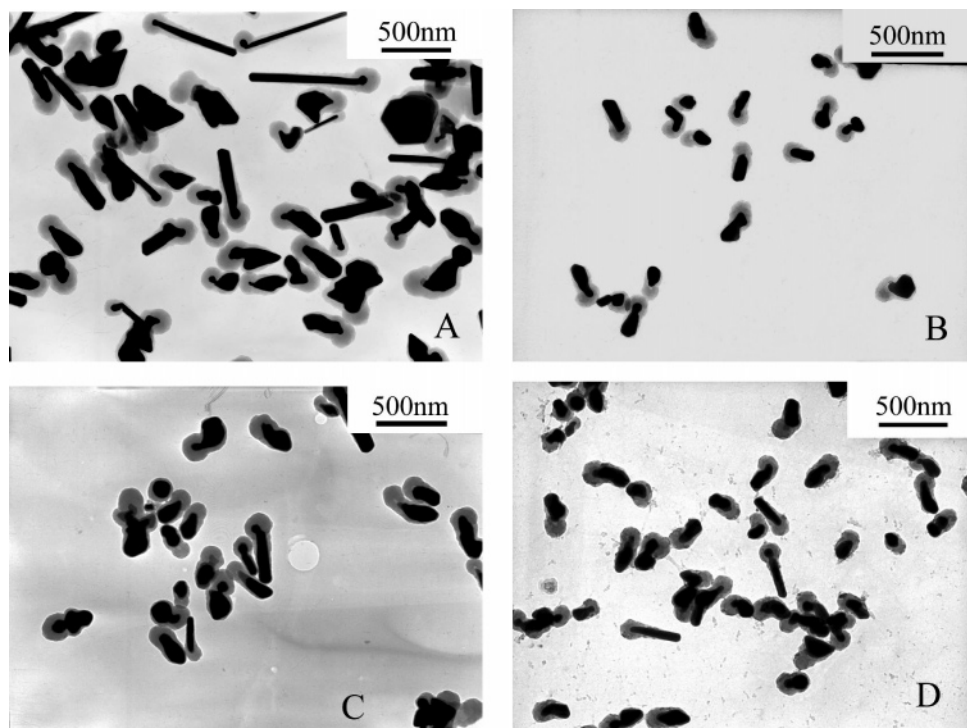


Figure 2. TEM images of PPy-coated Ag composites prepared at different molar ratios of AgNO₃ to pyrrole monomer: (A) 1, (B) 0.7, (C) 0.5, and (D) 0.25. Synthetic conditions: PVP concentration 2%; reaction time 48 h; room temperature.

range of sizes (Figure 1D). In the TEM images, it could be seen that the PVP concentration had less effect on the PPy shell thickness but had a strong effect on the Ag core diameter. It might be due to the different existent phases and interaction mechanisms.

Interface polymerization is an effective method to prepare conducting polymer nanostructures by using an immiscible organic/aqueous biphasic system.¹³ It has many advantages such as the process and purification are simple and the synthesis is easily scalable and reproducible. In this report, the two phases of CCl₄ containing pyrrole and water-dissolved AgNO₃ and PVP acted as the reactive biphasic system to prepare PPy-coated Ag nanocomposite. The dispersion degree of the as-prepared sample was very high with the help of the biphasic interface because the interface polymerization could also suppress the agglomeration of conducting polymer.

Herein, PVP as an anchor agent played an important role. The core–shell structure could not be formed without PVP. It is well-known that specific functional groups such as –CONH–, –SO₄^{2–}, and –C=O groups can be used to induce coating during the precipitation and surface reactions on the cores.¹⁴ PVP is a useful steric agent to promote a strong interaction between Ag particles and pyrrole monomer. For example, it has been used successfully in the preparation of uniform silica/PPy core–shell particles.¹⁵ The amphiphilic property of PVP would be beneficial for the adherence between the polymer shell and the inorganic core. Ag–O coordination could be formed through the pyrrolidone ring that was tilted on the surface of the silver.¹⁶ PVP with its dipolar imide group carries a fractional negative charge on the carbonyl oxygen.¹⁷ Polycationic PPy could react with PVP by an electrostatic effect. The adsorbed PVP might provide active sites on the Ag so as to induce the growing polycationic PPy chains to complete the coating of PPy layers. At the same time, PVP could prevent the aggregation of conducting polymer efficiently.¹⁸

In addition, the effect of the molar ratio of AgNO₃ to pyrrole monomer (represented by [AgNO₃]/[pyrrole]) on the resultant

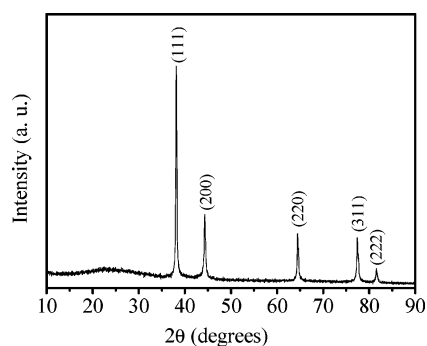


Figure 3. XRD pattern of PPy-coated Ag nanocomposite. Synthetic conditions: [AgNO₃]/[pyrrole] 0.7; PVP concentration 2%; reaction time 48 h; room temperature.

product was also studied. Figure 2 shows the TEM images of PPy-coated Ag nanocomposites synthesized at different [AgNO₃]/[pyrrole] values. When the value of [AgNO₃]/[pyrrole] was 0.7, the shell thickness and core diameter of the prepared composites were 10–150 and 100–300 nm, respectively (Figure 2B). PPy-coated Ag nanocomposite with a diameter of 150–400 nm was uniform in size and well dispersed. However, the size of Ag was increased and the shape became irregular when the ratio was increased from 0.7 to 1 or decreased from 0.7 to 0.5. Furthermore, some PPy could not form the coating layer when the ratio is decreased to 0.25.

The XRD pattern of the PPy-coated Ag nanocomposite prepared by interface polymerization is shown in Figure 3. XRD measurement confirmed the presence of Ag in the PPy/Ag composites. As shown in Figure 3, the weak reflection centered at a 2θ value of 24° was characteristic of the doped PPy.¹⁴ Another five diffraction peaks at 2θ = 38.1°, 44.2°, 64.5°, 77.3°, and 81.5° corresponded to Bragg's reflections from (111), (200), (220), (311), and (222) planes of Ag and were in good agreement with the reported data, showing the existence of Ag in the PPy/Ag composites.¹⁹

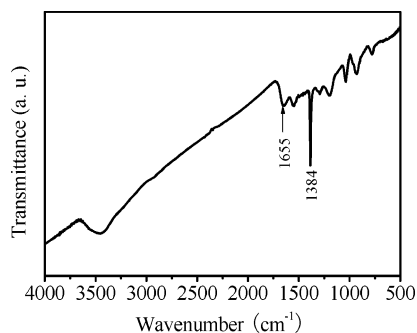


Figure 4. FTIR spectrum of PPY-coated Ag nanocomposite. Synthetic conditions: $[\text{AgNO}_3]/[\text{pyrrole}]$ 0.7; PVP concentration 2%; reaction time 48 h; room temperature.

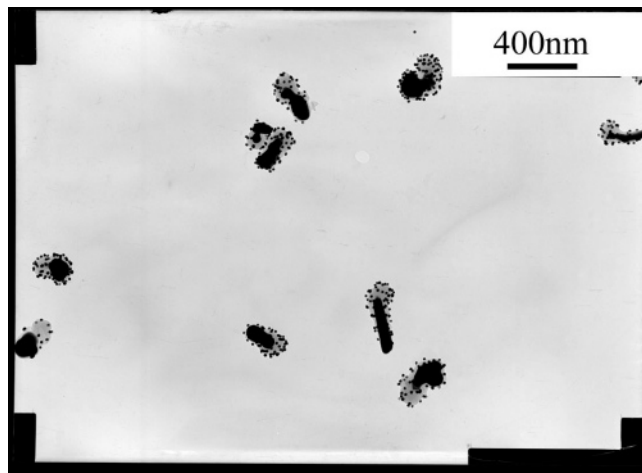


Figure 5. TEM image of three-layered Au-modified PPY-coated Ag nanocomposite. Synthetic conditions: $[\text{AgNO}_3]/[\text{pyrrole}]$ 0.7; PVP concentration 2%; reaction time 48 h; room temperature.

The molecular structures of the PPY-coated Ag nanocomposite were characterized by FTIR spectroscopy, as shown in Figure 4. In general, it can be seen that the characteristic PPY peaks are located at 1548 and 1477 cm^{-1} , due to the pyrrole ring stretching and the conjugated C–N stretching mode, respectively.²⁰ However, the band at 1477 cm^{-1} is very weak. The reason might be that the polymerization degree of PPY induced by AgNO_3 is low, or it is lack of observation caused by other strong absorptions. The peaks at 1294 and 1034 cm^{-1} are related to the in-plane vibrations of =C–H, 1188 cm^{-1} is assigned to the C–N stretching mode, and 775 cm^{-1} is attributable to C–H wagging vibration.²¹ In addition, the band at 1655 cm^{-1} corresponds to the stretching vibration of the C=O group, which indicates the presence of PVP in the resulting composites. Furthermore, a very strong absorption band assignable to NO_3^- is observed at 1384 cm^{-1} . This suggests that the obtained PPY in the PPY/Ag composite is doped by NO_3^- .

Three-layered Au/PPY/Ag composite was prepared through the reaction of PPY-coated Ag and Au colloidal solution. When the polycationic PPY was introduced into the Au colloid, Au-modified PPY/Ag composite was formed by an electrostatic effect because the surface of citrate-stabilized Au NPs was electronegative. TEM images provide the direct evidence of the adsorption of Au NPs on the PPY surface. The dark spot with a diameter of 30 nm Au NPs can be observed as shown in Figure 5. The amount of Au in the composite was determined by TGA. Because Au and Ag do not qualify as a loss under the experimental conditions, the residual weight percentage (wt %) can be referenced to the content of Au and Ag. Therefore, the content of Au can be calculated by subtracting the residual

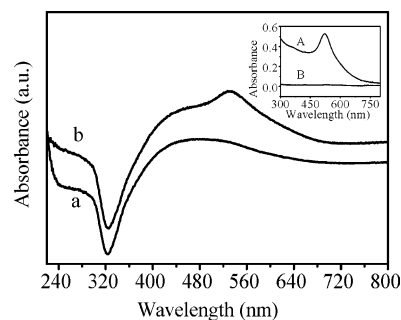


Figure 6. UV-vis spectra of (a) PPY/Ag and (b) Au/PPY/Ag. The insets show the UV-vis spectra of the as-prepared colloidal gold solution (A) and the gold solution after reaction with PPY and centrifugation (B). Synthetic conditions: $[\text{AgNO}_3]/[\text{pyrrole}]$ 0.7; PVP concentration 2%; reaction time 48 h; room temperature.

weight percentage of PPY/Ag from that of the Au/PPY/Ag. The residual weight percentage of PPY/Ag and Au/PPY/Ag is 40.2% and 45.3%, respectively. So the content of Au in the composite is 5.1%.

UV-vis absorption spectra of Au/PPY/Ag and PPY/Ag are shown in Figure 6. The insets show the UV-vis spectra of the as-prepared colloidal gold solution (A) and the gold solution after reaction with PPY and centrifugation (B). The characteristic peak of citrate-stabilized colloidal Au NPs appears at 522 nm. It is caused by the surface plasmon resonance. A great loss in the intensity of the surface plasmon resonance at 522 nm was found after Au NPs were deposited, indicating that Au NPs could be adsorbed on the PPY surface efficiently. The absorption intensity of the Au colloid is not affected by centrifugation. The fraction of Au in solution that can be deposited on PPY is up to 97%. This was calculated by subtracting the adsorption intensity of the gold solution at 522 nm after reaction with PPY and centrifugation (A1) from that of the prepared colloidal gold solution (A2) and then dividing by A2, that is, $(A2 - A1)/A2 \times 100\%$. The surface plasmon resonance peak of Au NPs was observed at 535 nm after Au NPs were combined with PPY, which was shifted to longer wavelengths compared to that of Au colloid solution. It indicated that there was a strong interaction between Au NPs and PPY. Meanwhile, the broad band at 460 nm was attributable to the $\pi-\pi^*$ transition of PPY chains that was well consistent with the reported data.²²

Dopamine (DA) is an important neurotransmitter in mammalian central nervous systems, and the loss of DA-containing neurons may lead to serious diseases including Parkinson's disease. The detection of DA has therefore been a subject of considerable interest. Since 1986, conducting polymers have been used to immobilize electrode to detect DA.²³ Along with the development of DA sensors prepared by conducting polymers, many effective efforts have been directed toward enhancing the selectivity and sensitivity.²⁴ Usually, the selectivity and sensitivity of DA sensors are higher in acidic condition. It is well-known that PPY bears good electrochemical behavior and has been applied to the field of chemically modified electrodes. In this work, Au/PPY/Ag composite was immobilized onto the surface of a GCE, which was taken as an example of developing a possible application as a DA biosensor. The GCE was previously tested in pH 1 H_2SO_4 solution before the Au/PPY/Ag and PPY/Ag composite were drop coated on it. It presented no redox process in the potential range studied. The working electrode coated with Au/PPY/Ag (PPY/Ag) was immersed in the electrolyte solution for 10 min prior to the measurement to ensure the diffusion of the solution to the interlayer space and permit better ionic exchange.

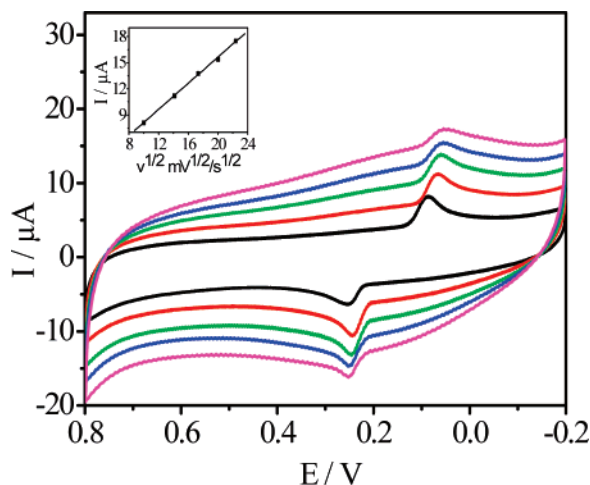


Figure 7. Cyclic voltammograms of Au/PPy/Ag-modified GCE measured in pH 1 H_2SO_4 solution at different scanning rates: from inner to outer 100, 200, 300, 400, 500 mV s^{-1} . The inset shows the calibration plot between the anodic peak current and the square root of the scanning rate. Synthetic conditions: $[\text{AgNO}_3]/[\text{pyrrole}]$ 0.7; PVP concentration 2%; reaction time 48 h; room temperature.

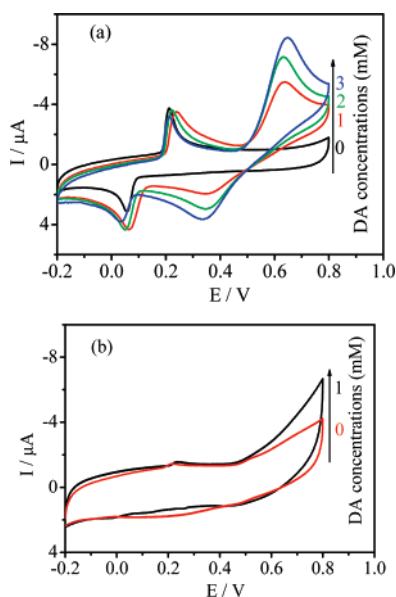


Figure 8. Cyclic voltammograms of (a) Au/PPy/Ag-modified GCE and (b) PPy/Ag-modified GCE in the absence and presence of different concentrations of DA at a scan rate 100 mV/s . Synthetic conditions: $[\text{AgNO}_3]/[\text{pyrrole}]$ 0.7; PVP concentration 2%; reaction time 48 h; room temperature.

The effect of the potential scanning rate (V) on the peak current for the Au/PPy/Ag-modified electrode was studied in the range of 100–500 mV/s , as shown in Figure 7. With the increase in scanning rate, the anodic peak potential shifts to a more positive direction and the cathodic peak potential shifts toward the more negative direction. The anodic peak current for PPy is increased linearly with the square root of the scanning rate ($V^{1/2}$), indicating that the peak current is diffusion controlled.²⁵

In the potential range of 0.8 and -0.2 V, the cyclic voltammograms (CV) of the Au/PPy/Ag-modified electrode in H_2SO_4 before and after the addition of DA are shown in Figure 8a. The CV curve of Au/PPy/Ag-modified electrode shows a pair of well-defined redox peaks, corresponding to the oxidation (anions move in) and reduction (anions move out) reaction of PPy. The redox peaks in the presence of DA appear at 635 and 358 mV for the Au/PPy/Ag-modified GCE,

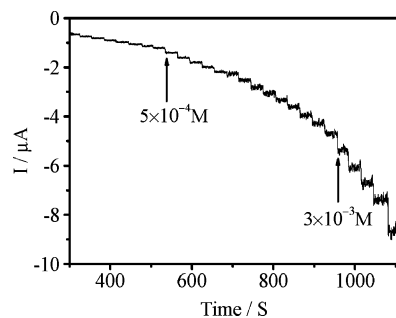


Figure 9. Typical steady-state response of Au/PPy/Ag-modified GCE on successive injection of different concentrations of DA into pH 1 H_2SO_4 solution while stirring with an applied potential of 635 mV . Synthetic conditions: $[\text{AgNO}_3]/[\text{pyrrole}]$ 0.7; PVP concentration 2%; reaction time 48 h; room temperature.

respectively, and are attributed to the oxidation/reduction of DA to dopaminequinone with participation of two electrons.²⁶ It can also be seen that the oxidation/reduction peak current is increased with the gradual addition of DA, showing the catalytic property of the modified electrode in the oxidation of DA. For comparison, the CVs of PPy-coated Ag composite without decoration of Au-modified electrode before and after the addition of DA are also studied (Figure 8b). As seen from the figure, the electrochemical activity and reversibility of PPy is not very good. Moreover, the catalytic anodic current of the PPy/Ag-modified GCE is observed at a more positive potential compared with that of Au/PPy/Ag-modified GCE, implying that the Au/PPy/Ag has a stronger catalytic effect on the oxidation of DA than that of PPy/Ag. Furthermore, the electrocatalytic anodic current in the Au/PPy/Ag system is about 7-fold higher than that in the PPy/Ag system. For example, at a DA concentration of 1 mM , the Au/PPy/Ag system generates an increased anodic current of 4.37 μA compared with the current without DA, whereas the PPy/Ag system yields an increased current of 0.61 μA .

According to our previous study, Au NPs can act as a catalyst for the oxidation of DA.²⁷ The electrocatalytic effect of Au on the oxidation of DA is different with the different size and amount of Au. When the size of Au is 30 nm, the catalytic efficiency is maximal. Therefore, Au NPs with the diameter is of 30 nm were used to modify PPy/Ag composite. The catalytic effect of Au NPs on the oxidation of DA can lead to the effective electrocatalytic oxidation of DA by Au/PPy/Ag-modified GCE. At the same time, the improved electrocatalytic oxidation of DA in the Au/PPy/Ag-modified electrode may also be due to the fact that the charge transport is enhanced through the Au/PPy/Ag composite system, which facilitates the electrical contacting of the DA with the electrode. The enhanced electron transfer in the Au/PPy/Ag system is attributed to the charge hopping through the metallic conductor Au NPs that mediates the effective charge migration through the polymer. It is well-known that Au is one important type of conductor. Although Au NPs do not make a continuous electron path, the incorporated Au NPs generate many active sites for charge transfer through the interface inside the electrode by making good contact with the PPy matrix. The effective transport of the electrons to the electrode in the Au/PPy/Ag matrix leads to the efficient electrocatalytic oxidation of DA and the electrochemical activity of PPy.

The current–time curve is recorded under the conditions of continuous stirring of the solution and successive step changes of DA concentration at 635 mV (as shown in Figure 9). When an aliquot of DA was added into 20 mL of H_2SO_4 , the reductive current rose steeply to reach a stable value. The time to reach

95% of the maximum current was within 7 s, which indicated a fast response process. The Au/PPy/Ag-modified GCE displayed increasing amperometric responses to DA with linear ranges from 1×10^{-4} to 5×10^{-3} mol/L, and the detection limit was 5×10^{-5} mol/L based on $S/N = 3$.

Conclusions

We have demonstrated the one-step synthesis of PPy-coated Ag nanocomposites in the presence of PVP by interface polymerization. This method has many advantages; for example, the process is simple, and synthesis is easily scalable and reproducible. Furthermore, the interface polymerization could also suppress the agglomeration of conducting polymer. When the percentage content of PVP was 2% and $[AgNO_3]/[pyrrole]$ was 0.7, the obtained composites with shell thicknesses of 10–150 nm and core diameters of 100–300 nm were uniform in size and well dispersed. The resulting composites were characterized by TEM, XRD, and FTIR. Au-modified PPy-coated Ag composite could be obtained through the reaction between PPy-coated Ag and Au colloidal NPs. The Au/PPy/Ag nanocomposite was immobilized on the GCE and applied to construct a DA biosensor. The Au/PPy/Ag-modified electrode showed an enhanced electrocatalytic activity for the oxidation of DA compared with PPy/Ag-modified electrode. This method could be extended to prepare other conducting polymer/inorganic nanocomposites with different compositions.

Acknowledgment. We greatly appreciate the support of the National Natural Science Foundation of China (Nos. 20325516, 20635020, 20521503), the National Basic Research Program of China (No. 2003CB615804), and Modern Analysis Center of Nanjing University.

References and Notes

- (1) Gangopadhyay, R.; De, A. *Chem. Mater.* **2000**, *12*, 608.
- (2) (a) Yan, F.; Xue, G.; Wan, F. *J. Mater. Chem.* **2002**, *12*, 2606. (b) Li, L.; Yan, F.; Xue, G. *J. Appl. Polym. Sci.* **2004**, *91*, 303.
- (3) Selvan, S. T.; Spatz, J. P.; Klok, H.; Möller, M. *Adv. Mater.* **1998**, *10*, 132.
- (4) Tian, S.; Liu, J.; Zhu, T.; Knoll, W. *Chem. Mater.* **2004**, *16*, 4103.
- (5) Marinakos, S. M.; Novak, J. P.; Brousseau, L. C. *J. Am. Chem. Soc.* **1999**, *121*, 8518.
- (6) Chen, A.; Wang, H.; Li, X. *Chem. Commun.* **2005**, 1863.
- (7) Sarma, T. K.; Chowdhury, D.; Paul, A.; Chattopadhyay, A. *Chem. Commun.* **2002**, 1048.
- (8) (a) Wu, C. G.; Bein, T. *Science* **1994**, *264*, 1757. (b) Martin, C. R. *Chem. Mater.* **1996**, *8*, 1739. (c) Martin, C. R. *Science* **1994**, *266*, 1961. (d) Huang, L.; Wang, Z.; Wang, H.; Cheng, X.; Mitra, A.; Yan, Y. *J. Mater. Chem.* **2002**, *12*, 388. (e) Wei, Z.; Zhang, Z.; Wan, M. *Langmuir* **2002**, *18*, 917. (f) Jang, J.; Yoon, H. *Chem. Commun.* **2003**, 720.
- (9) Zhang, X. Y.; Guox, W. J.; Manohar, S. K. *J. Am. Chem. Soc.* **2004**, *126*, 4502.
- (10) Liu, J.; Lin, Y.; Liang, L.; Voigt, J. A.; Huber, D. L.; Tian, Z. R.; Coker, E.; Mckenzie, B.; Mcdermott, M. J. *Chem. Eur. J.* **2003**, *9*, 605.
- (11) Huang, J. X.; Virji, S.; Weiller, B. H.; Kaner, R. B. *J. Am. Chem. Soc.* **2003**, *125*, 314.
- (12) Doron, A.; Katz, E.; Willner, I. *Langmuir* **1995**, *11*, 1313.
- (13) Huang, J.; Kaner, R. B. *J. Am. Chem. Soc.* **2004**, *126*, 851.
- (14) (a) Kojima, Y.; Usuki, A. A.; Kawasumi, M.; Okada, A.; Kurauchi, T.; Kamigaito, O. *J. Polym. Sci., Part A: Polym. Chem.* **1993**, *31*, 983. (b) Seo, I.; Pyo, M.; Cho, G. *Langmuir* **2002**, *18*, 7253.
- (15) Hao, L. Y.; Zhu, C. L.; Chen, C. N.; Kang, P.; Hua, Y.; Fan, W. C.; Chen, Z. Y. *Synth. Met.* **2003**, *139*, 391.
- (16) Gao, Y. *J. Phys. Chem. B* **2004**, *108*, 12877.
- (17) Murugesan, R.; Anitha, G.; Subramanian, E. *Mater. Chem. Phys.* **2004**, *85*, 184.
- (18) (a) Somani, P. R. *Mater. Chem. Phys.* **2002**, *77*, 81. (b) Ghosh, P.; Siddhanta, S. K.; Chakrabarti, A. *Eur. Polym. J.* **1999**, *35*, 699.
- (19) Zhang, Z. P.; Zhang, L. D.; Wang, S. X. *Polymer* **2001**, *42*, 8315.
- (20) (a) Cho, G.; Fung, B. M.; Glatzhofer, D. T.; Lee, J. S.; Shul, Y. G. *Langmuir* **2001**, *17*, 456. (b) Jang, J.; Oh, J. H. *Adv. Funct. Mater.* **2005**, *15*, 494.
- (21) Mathis, G. I.; Troung, V. T. *Synth. Met.* **1997**, *89*, 103.
- (22) (a) Chen, A.; Kamata, K.; Nakagawa, M.; Iyoda, T.; Haiqiao, W.; Li, X. *J. Phys. Chem. B* **2005**, *109*, 18283. (b) Selvan, S. T.; Spatz, J. P.; Klok, H.; Möller, M. *Adv. Mater.* **1998**, *10*, 132. (c) Ojio, T.; Miyata, S. *Polym. J.* **1986**, *18*, 95.
- (23) Saraceno, R. A.; Pack, J. G.; Ewing, A. G. *J. Electroanal. Chem.* **1986**, *197*, 265.
- (24) (a) Gao, Z.; Yap, D.; Zhang, K. *Anal. Sci.* **1998**, *14*, 1059. (b) Erdogdu, G.; Ekin, E.; Karagozler, A. *Polym. Bull.* **2000**, *44*, 195. (c) Ferreira, M.; Dinelli, L.; Wohnrath, K.; Batista, A.; Oliveira, O. *Thin Solid Films* **2004**, *446*, 301. (d) Jiang, L.; Xie, Q.; Li, Z.; Li, Y.; Yao, S. *Sensors* **2005**, *5*, 199.
- (25) Zakharchuk, N. F.; Meyer, B.; Hennig, H.; Scholz, F.; Stojek, A.; Jaworski, Z. *J. Electroanal. Chem.* **1995**, *398*, 23.
- (26) Lin, X.-Q.; Zhang, L. *Anal. Lett.* **2001**, *34*, 1585.
- (27) Feng, X. M.; Mao, C. J.; Yang, G.; Hou, W. H.; Zhu, J.-J. *Langmuir* **2006**, *22*, 4384.